The plug domain of FepA, a TonB-dependent transport protein from *Escherichia coli*, binds its siderophore in the absence of the transmembrane barrel domain

Ken C. Usher*†, Engin Özkan†, Kevin H. Gardner†, and Johann Deisenhofer*†‡

*Howard Hughes Medical Institute and †Department of Biochemistry, University of Texas Southwestern Medical Center, 5323 Harry Hines Boulevard, Dallas, TX 75390

Contributed by Johann Deisenhofer, July 11, 2001

FepA, an outer membrane iron siderophore transporter from *Escherichia coli*, is composed of a 22-stranded membrane-spanning β barrel with a globular N-terminal ''plug'' domain of 148 residues that folds up inside the barrel and completely occludes the barrel's interior (1). We have overexpressed and purified this plug domain by itself and find that it behaves *in vitro* as a predominantly unfolded yet soluble protein, as determined by circular dichroism, thermal denaturation, and NMR studies. Despite its unfolded state, the isolated domain binds ferric enterobactin, the siderophore ligand of FepA, with an affinity of 5 μM, just 100-fold reduced from that of intact FepA. These findings argue against the hypothesis that the plug domain is pulled intact from the barrel during transport *in vivo* but may be consistent either with a model where the plug rearranges within the barrel to create a channel large enough to allow transport or with a model where the plug unfolds and comes out of the barrel.

Iron import is often the limiting factor in bacterial growth, largely because of insolubility of Fe(III). As a consequence, microorganisms have developed high-affinity systems to scavenge whatever iron is available from the surrounding medium. One such pathway that is used by *Escherichia coli* involves uptake of a siderophore, ferric enterobactin (Fe-ent), by a series of gene products from the Fep operon. *E. coli* synthesizes and secretes enterobactin, a tricatecholate compound that has an extremely high affinity for Fe^{3+} ions (2). It captures exogenous Fe^{3+} by forming a complete six-ligand coordination sphere around the iron (3). Fe-ent is specifically recognized by FepA, an *E. coli* outer membrane protein that imports it into the periplasm. Fe-ent is subsequently bound by a periplasmic binding protein, FepB, and transported across the inner membrane by the FepCDG complex. The FepCDG complex is an ATP-dependent ABC transporter, but the overall process is limited by the ability of FepA to carry out active transport (4) with the assistance of inner membrane proteins TonB and ExbBD and the inner membrane chemiosmotic proton gradient (5).

FepA is a member of a family of outer membrane proteins classified as TonB-dependent receptors on the basis of the presence of a short consensus sequence near the N terminus known as the TonB box, with which TonB physically interacts (6). These receptors recognize and import specific compounds, mainly siderophores, that are too large to go through passive diffusion porins and require transport against a concentration gradient. FepA recognizes Fe-ent, which is secreted by *E. coli*; other members of this receptor family in *E. coli* include FhuA, which imports ferrichrome, a siderophore secreted by fungi, and BtuB, which imports vitamin B. Most of the receptors are also used as the recognition and entry points for different colicins and bacteriophage, often in a way that requires the action of TonB. TonB-dependent receptors compete for a limited number of TonB molecules (7), suggesting that the TonB molecule recognizes a change in the receptor conformation at the inner side of the membrane on siderophore binding. After this event, TonB uses energy from the chemiosmotic potential of the inner membrane to effect a conformational change in the outer membrane receptor that results in active transport, then dissociates from the receptor at the end of the cycle, freeing it to interact with other receptor molecules (Fig. 1).

The crystal structure of FepA (1) shows that its TonB box is on the periplasmic side of the membrane, part of the 150-aa N-terminal globular domain that fills the interior of the large membrane-spanning β barrel of FepA (Fig. 2*A*). This barrel, which consists of 22 antiparallel strands, has large extracellular loops. It can be seen in crystal structures of the related FhuA protein bound to its siderophore (8, 9) that the siderophore binds to sites where it contacts some of the outer loops as well as several residues from the N-terminal plug domain. Crystal structures of FhuA with and without its siderophore bound show very little change near the binding site but large changes at the N terminus of the protein, 30 Å away on the inner face of the membrane. In the ligand-bound structure, a short helix (residues 24–29) unwinds and changes the position of the N terminus of the visible part of the protein. In both FhuA structures, residues 1–19, including the TonB box, cannot be seen, however. The structure of FepA, in which the siderophore is not tightly bound, shows the TonB box residues ordered and located in a different position than any of the FhuA structures would suggest. Movement of the TonB box in response to ligand binding, such as that seen between different FhuA structures, may be the signal that initiates action by TonB.

Crystal structures cannot directly show the critical siderophore transport step itself, particularly because TonB, a necessary *in vivo* component, resides in a different membrane than the receptor and would need an intact membrane to have the chemiosmotic potential that is required for transport to occur. None of the published structures contain an open channel through or around the N-terminal plug domain that fills the barrel's interior, yet Fe-ent is a roughly spherical molecule with a minimum diameter of 10 Å. Two possible models for how passage is made are that TonB causes a rearrangement of the plug domain within the barrel or that TonB pulls the plug domain out of the barrel entirely (1). Each proposal has drawbacks: it is not clear how there might be enough space available for the plug to sufficiently rearrange within the barrel to allow a siderophore

Abbreviations: Fe-ent, ferric enterobactin; FepA150, residues 1–148 of FepA protein; HSQC, heteronuclear single quantum coherence; CD, circular dichroism.

‡To whom reprint requests should be addressed. E-mail: Johann.Deisenhofer@utsouthwestern.edu.

The publication costs of this article were defrayed in part by page charge payment. This article must therefore be hereby marked "*advertisement*" in accordance with 18 U.S.C. §1734 solely to indicate this fact.

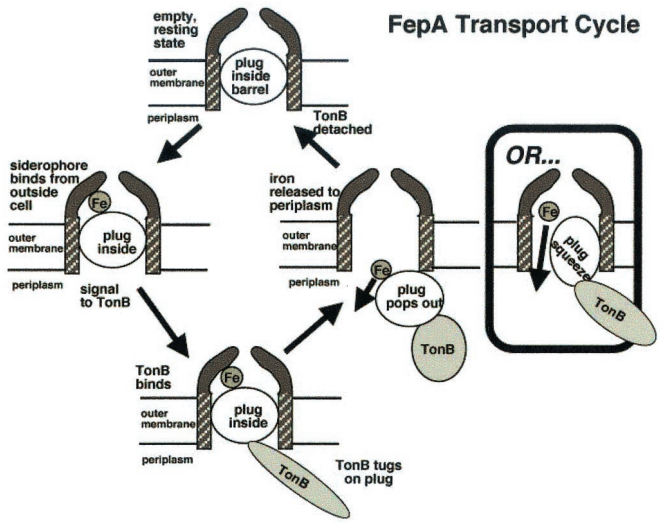

Fig. 1. Schematic diagram illustrating critical steps in the transport cycle of siderophores by FepA or other TonB-dependent receptors, including two possible ways to open a large transmembrane channel.

to pass by, whereas removal of the plug would require disruption of a large shared surface between the plug and barrel. Plug removal could also explain entry of colicins or bacteriophage DNA that use TonB-dependent receptors as recognition points; there is no direct evidence to tell whether these pass through the barrel or directly pierce the adjacent outer membrane bilayer, but they are even larger than the siderophores and depend not only on the receptor itself but also on the presence of a functional TonB complex (10). This paper investigates physical properties of the plug domain alone, as it may exist if it is removed from the barrel during the transport cycle.

Materials and Methods

A plasmid-encoded copy of the *E. coli* fepA gene (GenBank accession no. M13748) (11) was used to clone its N-terminal part via PCR, by using primers that selected the native signal peptide and the first 148 amino acids of the mature protein. The primers were also designed to add a six-histidine affinity tag and a stop codon at the carboxyl terminus, as well as *Nde*I and *Hin*dIII restriction sites just outside the coding region. The resulting product was agarose gel-purified and ligated by using the Invitrogen TA cloning kit into the pCR2.1 vector. Dideoxy DNA sequencing with an ABI automated sequencer (Applied Biosystems) was performed from T7 and M13R sequencing primers outside the insert region to verify that it matched the published sequence. The insert was excised with restriction enzymes and ligated into the multiple cloning site of the pET17b expression vector (Novagen), which then was transformed into *E. coli* strain BL21-DE3(pLysS) (Novagen) for overexpression. Cultures were grown in Luria–Bertani medium (12) containing 0.1 μg/ml of carbenicillin. Expression was induced by addition of 100 μM isopropyl-β-D-thiogalactopyranoside (IPTG) to actively growing cultures having an OD_{600} near 0.5 and allowed to grow an additional 4 h before harvesting by centrifugation. Cell pellets were resuspended in a 50% (wt/vol) mixture with a lysis buffer containing 1 mg/ml of chicken egg white lysozyme (Sigma), 50 mM Tris (pH 8.0), protease inhibitor mixture (one tablet per 100 ml of buffer, Boehringer Mannheim), 50 mM NaCl, and 6% glycerol, then sonicated while chilled on wet ice to lyse them. After lysis, 40 mg of protamine sulfate (Sigma) dissolved in water was added to precipitate nucleic acids. Cell debris were spun down by centrifugation at 25,000 $\times$ *g* for 60 min. The supernatant solution was run over a 1-ml nickel triacetate (Qiagen, Chats-

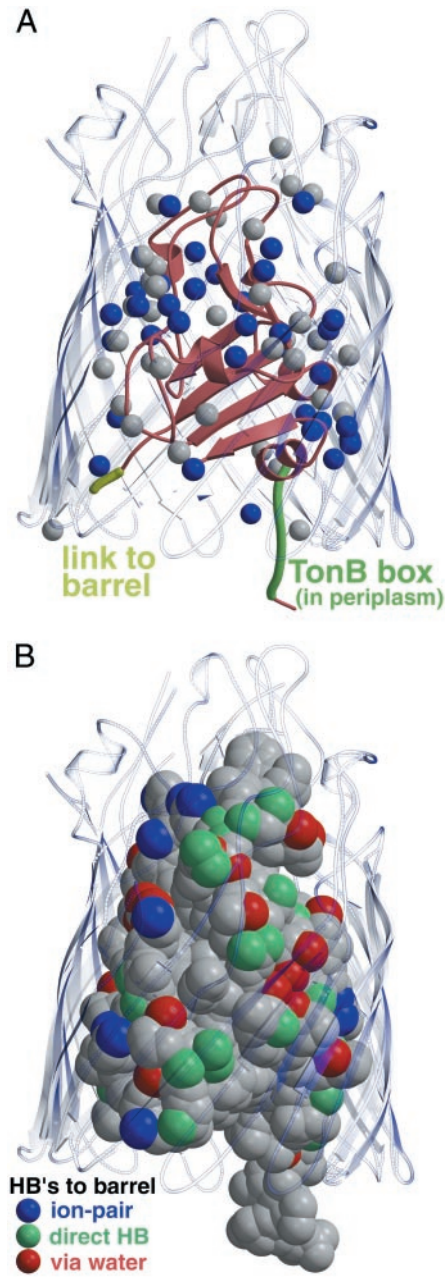

Fig. 2. A ribbon diagram of the crystal structure of FepA (Protein Data Bank ID code 1FEP), with the membrane-spanning β barrel and its loops shown as transparent. Figures were produced by using BOBSCRIPT (30) and rendered by using RASTER3D (31). (*A*) Plug domain of FepA (residues 1–148) is shown in red, with residue 148, the last residue expressed in FepA150, highlighted in yellow, and residues 12–18, the conserved TonB interaction box, highlighted in green. Blue spheres represent bound solvent molecules making bridging hydrogen bonds between the barrel and the plug domains (3.5 Å or less from each); white spheres represent other bound solvent molecules near the interface (3.5 Å or less from one domain and 3.5–5 Å from the other). (*B*) Plug domain of FepA is shown as a CPK representation, highlighting atoms on the surface of the plug domain that make bridging polar interactions to the inner surface of the β barrel. Red spheres represent polar atoms that make hydrogen bonds to bound water molecules that in turn make other hydrogen bonds to atoms of the barrel. Blue spheres are charged sidechain atoms from Arg, Lys, Asp, or Glu that form salt bridges with oppositely charged sidechains on the barrel. Green spheres are other donor or acceptor atoms that form hydrogen bonds directly with polar atoms on the barrel.

worth, CA) column to bind the desired protein via its 6-histidine tag, washed with 50 ml of buffer containing 50 mM imidazole to remove weakly binding contaminants, then eluted by using 10 ml of buffer with 150 mM imidazole. The eluate was then bound to a methylsulphonate cation exchange column (MonoS 5/5 column, Amersham Pharmacia FPLC system) and eluted by a sodium chloride gradient at about 0.2 M concentration, in 6% glycerol and 50 mM Hepes buffer, pH 7.4. A 10-ml Amicon gas filtration unit was used to exchange buffers and subsequently to concentrate the protein to the desired level. The protein was identified by SDS/PAGE, by DNA sequencing of the plasmid insert, and by sequencing via Edman degradation of the first six amino acids of the overexpressed protein. Gel filtration chromatography was carried out by using a Superose12 column (Amersham Pharmacia FPLC system) equilibrated in 50 mM NaCl and 50 mM tricine buffer, pH 8.0. All purification steps were carried out at 4°C. ^{15}N-labeled protein was prepared similarly, except that cells were grown in minimal M9 medium (12) prepared with ^{15}N-labeled ammonium chloride and with 1 mM magnesium sulfate added.

Circular dichroism (CD) was measured by using an Aviv 62DS (Aviv Associates, Lakewood, NJ) instrument, with a protein concentration of 9 μM in a buffer of 100 mM sodium fluoride and 10 mM sodium phosphate, pH 7.3, in a closed quartz cuvette having a path length of 1 mm. Five repeats of a wavelength scan from 190 to 250 nm were performed at 4°C, with a 3-sec averaging time per data point. Subsequently, the sample was heated from 4 to 80°C at a rate of 2°C per minute, while monitoring the CD signals at 196, 208, and 218 nm.

One-dimensional proton NMR spectroscopy was performed at 25°C by using a Varian 500 Hz spectrometer. The NMR pulse sequence used water suppression by gradient-tailored excitation (WATERGATE, ref. 13). Protein concentration was 100 μM in 90 mM sodium fluoride and 10 mM sodium phosphate buffer, pH 6.7, also containing 10% D_2O. After the initial spectrum, Fe-ent was added to concentrations of 20 μM, then 200 μM, and further spectra were collected. Two-dimensional ^{15}N-^{1}H heteronuclear single quantum coherence (HSQC) NMR spectra (14) were acquired under the same conditions on a 600 MHz spectrometer, by using a 200-μM sample of ^{15}N-labeled residues 1–148 of FepA protein (FepA150) and 0-, 40-, and 240-μM concentrations of Fe-ent. The NMR titration was repeated by using ferrichrome, a siderophore that is not transported by FepA, with a 100-μM sample of ^{15}N-labeled FepA150 and 0-, 60-, and 210-μM concentrations of ferrichrome. Finally, NMR titration was repeated a third time by using gallium enterobactin, in which the siderophore is loaded with a metal ion, Ga^{3+}, having the same charge and similar properties as Fe^{3+} (3), except that gallium is not paramagnetic. A 150-μM sample of ^{15}N-labeled FepA150 was titrated successively with 0-, 30-, 90-, and 180-μM concentrations of gallium enterobactin.

Fluorescence polarization was measured at 25°C by using a Photon Technology International (Lawrenceville, NJ) fluorescence spectrophotometer and FELIX data collection software. For each sample, 10 1-sec measurements were made in each of four polarizer combinations, and a correction was calculated to compensate for any differences in the transmission of the excitation and emission polarizers (15). Fluorescence polarization was measured by using an excitation wavelength of 330 nm and an emission wavelength of 495 nm, first for 20 μM Fe-ent in solution, then for several concentrations of a 1:1 mixture of Fe-ent and FepA150, at concentrations of 200, 20, 10, and 5 μM of each component.

Buried surfaces and polar interactions were calculated for the plug domain of intact FepA by using the program EDPDB (16), with a probe radius of 1.4 Å for surface calculations and a distance cutoff of 3.5 Å for polar interactions.

Table 1. Percentage frequencies of hydrophobic, polar, and charged residues in different environments in the plug domain of FepA, compared with other proteins

	Percentage frequencies		
Amino acids	Exterior	Interface	Interior
Hydrophobic	32 (41)	31 (47)	83 (71)
Polar	36 (29)	35 (23)	13 (23)
Charged	32 (30)	34 (22)	4 (6)

Following ref. 18, Ala, Gly, Ile, Leu, Met, Phe, Pro, and Val were classed as hydrophobic, Asn, Cys, Gln, His, Ser, Thr, Trp, and Tyr as polar, and Asp, Arg, Lys, and Glu as charged. Percentages reported for the 23 protein dimers used in the Jones and Thornton study (18) are shown in parentheses.

Results

Analysis of the crystal structure of FepA shows that, whereas the plug domain makes extensive interactions with the barrel that encloses it, the interface is not particularly hydrophobic. The surface area of the plug that is buried by interaction with the barrel is 5,080 Å^2, including 2,740 Å^2 (54%) carbon atoms. The barrel surface buried by the plug domain is 4,400 Å^2, including 1,980 Å^2 (45%) carbon atoms. Comparing these figures with percentages of nonpolar atom surfaces calculated for protein interiors (61–74%) and exteriors (50–63%) (17) and for interfaces between proteins (68%) (18) suggests that the buried surface of the plug domain looks more similar to protein exterior surfaces than to most interior buried surfaces. The difference in total buried surface of the plug over the complementary barrel surface is unremarkable and is caused mainly by the concavity of the inner barrel surface. Analysis of the basis of the types of sidechains found on the exterior, interface, and interior of the plug domain following the protocol of Jones and Thornton (18) is shown in Table 1. The results show that the interior of the plug domain is predominantly made up of hydrophobic sidechains, as expected for globular proteins, but the barrel interface and the exterior of the domain have mostly polar and charged sidechains, to an extent similar to or even greater than what is typical for the exterior of globular proteins. The hydrophobicity pattern found for the plug domain suggests that it might be stable on its own as a folded globular protein in solution.

There are 65 direct hydrogen bonds (donor and acceptor atoms within 3.5 Å of each other) between the plug and the barrel, including 15 salt bridge interactions between negatively charged Asp or Glu sidechains and positively charged Arg or Lys sidechains (Fig. 2*B*). Although hydrogen bonds must form in any folded protein, they are thought not to be the dominant force favoring protein stability and may in fact oppose folding (19), because a protein's polar groups can hydrogen bond with water molecules in the unfolded state. Even so, the hydrogen bonds may pose a substantial kinetic barrier to removal or insertion of the plug domain in the barrel, because each one would need to be broken and the donors and acceptors solvated with water. One factor in the FepA transport system that might aid this process is that already 40 bound water molecules are visible in the x-ray structure that bridges the plug and the barrel, making hydrogen bonds with each part (Fig. 2*A*). Also, TonB is known to use energy to facilitate transport, possibly by applying mechanical force on the part of the plug with which it interacts to help break hydrogen bonds transiently.

Overexpression and purification of FepA150 from 6 liters of *E. coli* culture produced about 10 g of wet cell pellet, resulting in 4 mg of purified protein. After nickel chelation and cation exchange chromatography, the protein eluted as a single peak from a gel filtration column, indicating that it exists in a soluble monodisperse state under the conditions studied. It eluted at a volume between those obtained for two globular protein stan-

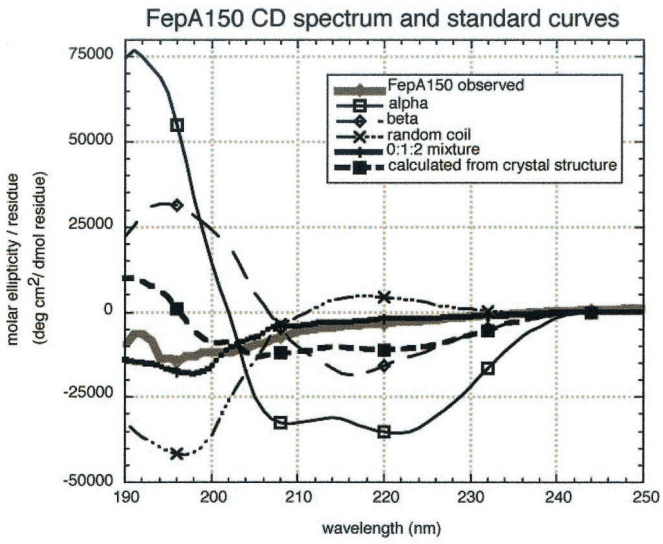

Fig. 3. FepA plug domain CD spectrum(◆), measured at 4°C, along with standard curves measured for poly-L-lysine under different conditions to represent helical (□), extended (◇), and random coil (X) conformations (20) and linear combinations of those curves in a 0.0:0.33:0.67 mixture (+) that mimics the observed CD spectrum and in a 0.28:0.21:0.51 mixture (■) that represents a calculated spectrum based on the plug domain conformation from the crystal structure of intact FepA.

dards, ovalbumin (molecular mass 43 kDa) and carbonic anhydrase (molecular mass 30 kDa). Because the actual molecular mass of FepA150 is just 17 kDa, this result indicates either that it associates as a folded globular dimeric protein, or that it has a hydrated random coil conformation, which would occupy a larger volume and thus elute more quickly than a globular protein of equivalent mass. Other results reported below demonstrate that in this case the latter option, elution as a random coil, is most likely.

The CD spectrum of FepA150 is shown in Fig. 3. The observed spectrum is not the same as that shown for standard random coil peptides (20), suggesting that it might have some secondary structure. For comparison, a hypothetical spectrum based on a 1:2 linear combination of the standard curves for extended and random coil peptide conformations (20), which appears to match the observed spectrum closely, is shown. The CD spectrum calculated by using the observed secondary structure of each residue in the crystal structure of the domain from the intact FepA protein (Fig. 3) matches less well. Altogether, the observed spectrum suggests that the domain is in neither a strictly random conformation nor the folded conformation observed in the crystal structure of intact FepA, and that most of the residues have no regular secondary structure. CD spectra similar to that seen for FepA150 have previously been taken as evidence for intrinsically unstructured states of other proteins such as synaptobrevin and SNAP-25 (21) and several fibronectin-binding domains (22). Temperature scans of CD signals at 196, 208, and 218 nm (data not shown) exhibit no significant or cooperative changes in the range from 4 to 80°C, suggesting that no temperature-dependent unfolding (at least none that alters secondary structure) occurs on heating, i.e., that the domain is already unfolded.

The HSQC NMR spectrum of ^{15}N-labeled FepA150 (Fig. 4) reveals only limited chemical shift dispersion of the amide protons, unlike what is seen in folded proteins because of secondary and tertiary structure interactions (23). Most of the primary amide protons of FepA150 are clustered between 7.9 and 8.5 ppm in ^{1}H and 112–125 ppm in the ^{15}N dimension. Additional peaks corresponding to glycine residues, of which there are 16 in FepA150, are seen with ^{15}N chemical shifts in the 107–112 ppm range. The intense clusters of peaks seen at 7.7 and 6.9 ppm in ^{1}H (112 ppm in ^{15}N) are where they would be expected for surface-exposed asparagine and glutamine side chains in the protein. The two small downfield peaks near 10.2 ppm (130 ppm in ^{15}N) represent the indole protons of the two tryptophan residues in FepA150 and are at the position expected for surface-exposed residues. Six amide proton peaks (labeled in Fig. 4) are significantly shifted downfield from the region where the other backbone amides are clustered. The ^{1}H chemical shifts of these peaks strongly suggest that they participate in secondary structure in an extended conformation (23). However, the low intensity of these peaks (≈10–20% of the Trp indole NH), suggests they exist only in part of the population of molecules of the sample, so that even this small segment of secondary structure is only partially formed.

Analysis of one-dimensional ^{1}H NMR spectra of FepA150 (data not shown) supports our conclusions above. Several peaks are observed upfield of 0.5 ppm, likely from methyl protons in unique environments generated by tertiary interactions. However, the overall chemical shift dispersion of these spectra is poor, consistent with the presence of little stable tertiary structure.

The structural effects of siderophore/FepA interactions were investigated by titrating ^{15}N-labeled FepA150 with increasing concentrations of Fe-ent. The addition of Fe-ent led to the weakening of many resonances, likely because of broadening effects caused by interactions with the paramagnetic iron of the siderophore (Fig. 4). This occurred even with substoichiometric amounts (40 vs. 200 μM FepA150) of Fe-ent and worsened when a slight excess (240 μM) was added. Some resonances (including the Trp A indole NH) disappeared entirely in the first step, others became smaller (including the Trp B indole NH), then disappeared when excess Fe-ent was added, whereas still others remained visible even with excess Fe-ent, although they appeared much weaker than in the original spectrum collected without any Fe-ent. No instances of new or shifted peaks were observed arising from addition of Fe-ent in either the one- or two-dimensional HSQC spectra.

The observation that the NMR spectrum of FepA150 was greatly weakened by addition of Fe-ent, with some resonances disappearing much earlier than others, has two possible explanations. Fe-ent might act simply through nonspecific proximity of the paramagnetic iron to the protein in solution, causing resonances to be broadened and disappear, with interior protons of a somewhat compact FepA150 polypeptide being less immediately accessible to the bulky Fe-ent molecule than others on the surface. Alternatively, FepA150 specifically binds Fe-ent, even though the protein appears largely unfolded, and resonances within or close to the binding site are much more strongly affected by broadening than those farther away from it. To distinguish between these possibilities, spectra were collected on a second sample of ^{15}N-labeled FepA150, titrated with similar concentrations of ferrichrome, a siderophore of similar size but dissimilar structure (2) that is not recognized by intact FepA. These spectra showed a mild reduction in the intensity of the HSQC spectra, but all of the peaks were reduced approximately equally. Even in excess ferrichrome, the spectrum intensity was reduced by less than 50%, and all of the peaks lost height to a similar extent, suggesting strongly that this milder broadening is what one would find from a nonspecific proximity of siderophore and protein, whereas the much stronger effect seen with Fe-ent and FepA150 is because of a specific interaction.

HSQC spectra of ^{15}N-labeled FepA150 (data not shown) showed very little change on addition of gallium enterobactin, a nonparamagnetic analog of Fe-ent. The Trp A and B indole NH peaks decreased slightly in intensity but remained present even

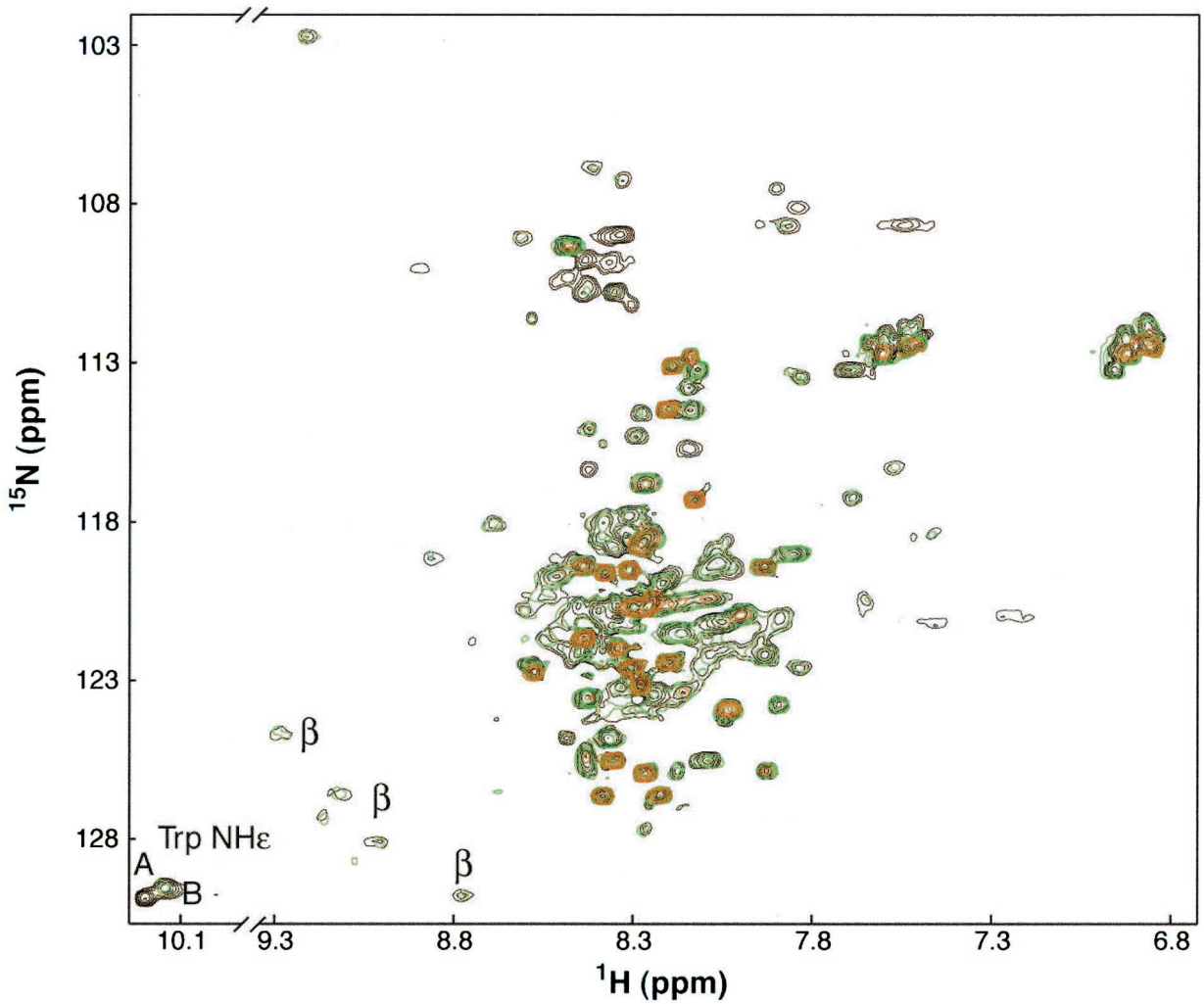

Fig. 4. 15N-^{1}H HSQC spectrum of uniformly ^{15}N-labeled FepA plug domain (concentration 200 μM). Peaks shown in black were measured in the absence of Fe-ent, whereas the green peaks had 20 μM Fe-ent added and the red ones 240 μM Fe-ent. Labels Trp A and B indicate two indole proton peaks referred to in the text, whereas the six small peaks closest to the notation "β" are backbone amide protons whose chemical shifts suggest them to be in an extended conformation/secondary structure (23).

when excess gallium enterobactin was added. No broadening or disappearance of peaks was observed. Provided that gallium enterobactin behaves similarly to Fe-ent, this result confirms that the broadening seen earlier on addition of Fe-ent was because of proximity of the paramagnetic iron to the protein. Lack of significant chemical shift changes among the protein's amide protons on addition of gallium enterobactin could indicate that it did not bind to FepA150, but the marked difference between the Fe-ent and ferrichrome results argues that FepA150 does indeed bind Fe-ent, and this binding is further explored in the fluorescence polarization experiment described next.

To confirm and quantify the binding seen by NMR between FepA150 and Fe-ent, fluorescence polarization of Fe-ent alone was measured and compared with its polarization in equimolar mixtures with FepA150 at several concentrations, as summarized in Table 2. The polarization depends on the rate of tumbling of the fluorophore in solution and will increase when it is bound to protein molecule, making it part of a larger particle that will reorient more slowly. A marked difference in polarization is seen for Fe-ent with and without FepA150 present, indicating that it does bind to the protein. The decrease in polarization seen in the 5- to 20-μM concentration range reflects the presence of a substantial fraction of unbound Fe-ent at these concentrations, corresponding to a K_d of about 5 μM.

Discussion

Although analysis of the plug domain's structure suggests that it would be reasonable for it to remain folded in the absence of the FepA barrel, and that it might do so during the course of the Fe-ent import cycle, the experimental evidence described here

Table 2. Fluorescence polarization measurements of a 1:1 mixture of Fe-ent and FepA150, using Fe-ent as the fluorophore, with an excitation wavelength of 330 nm and an emission wavelength of 445 nm

[Fe-ent], μM	[FepA150], μM	Polarization	Apparent K_d, μM
20	0	.007 ± .01	Unbound
5	5	.22 ± .15	3.8
10	10	.26 ± .09	5.6
20	20	.40 ± .09	4.5
100	100	.52 ± .08	Assumed fully bound

suggests otherwise. The plug domain was expressed and purified by itself, N-terminal amino acid sequencing verified that its signal peptide was processed just as is seen for the wild-type FepA, and gel filtration chromatography demonstrated that it behaves as a monodisperse soluble species in a detergent-free aqueous environment. However, results from CD and NMR show that the domain is predominantly unfolded under the conditions studied, although there is also evidence for a small remnant of structure in some of the FepA150 molecules. A number of protein domains are known that are intrinsically unfolded until they interact with another protein (24, 25) where the folded/unfolded transition is part of the natural role of the protein (26). This could be the case for the plug domain of FepA: it could come out of the barrel during siderophore transport in response to inputs from siderophore binding and from TonB, unfolding itself as it does so.

The instability of FepA150 and the polar hydrated nature of the plug domain interactions with the barrel seen in the crystal structure may indicate that, despite its apparently globular shape, it is only marginally stable and is poised to unfold and come out of the barrel during transport. Unfolding of the main part of the plug domain would necessarily provide a favorable increase in conformational entropy, whereas loss of internal interactions should produce an opposing enthalpic cost, and changes in bound water interactions could produce a variety of contributions. The experimental results here suggest that all those thermodynamic terms in plug removal and unfolding may be very close to being balanced, which is just what would be needed for that to occur during transport, with assistance from energized TonB. The probable kinetic mechanism of this is unclear but might involve the bound water seen at the barrel-plug interface. FepA also acts as the entry point for colicins B and D (27), and a mechanism that involves unfolding and removal of the plug domain would explain the dependence of these elongated (28) but bulky molecules (55 kDa; ref. 29) on TonB-dependent receptors, because it would transiently open a large channel, around 30 Å in diameter, for them to pass through. The current experiments are not conclusive, however, and it remains quite possible that the plug does not come out of the barrel at all, but instead undergoes a major conformational rearrangement within the barrel to form a channel large enough to allow the Fe-ent molecule to pass by, and that larger objects such as colicins cross the membrane by some other mechanism despite their dependence on FepA and TonB.

The observation that FepA150, despite its predominantly unfolded state, retains a binding affinity for Fe-ent that is only 100-fold reduced from the 50 nM K_d of intact FepA (1) was unexpected but is consistent with its retaining biological function outside of the barrel. Although FepA150 is shown to be predominantly unfolded, the residual structure that is seen may cluster near the putative siderophore-binding loops, near residues Arg-66 and -102. If the domain is removed from the barrel into the periplasm during the transport cycle, having a lesser affinity for Fe-ent in the periplasm could be a useful feature, facilitating transfer of the siderophore to the periplasmic binding protein, FepB, whereas the resting state of FepA with the plug inserted in the barrel retains a high affinity for extracellular Fe-ent.

We thank Drs. Josep Rizo and Philip J. Thomas for carefully reading the manuscript and for constructive criticism, Mss. Yoga Chelliah and Maya Palnitkar for help with protein expression and purification, and Ms. D. B. Staber for help with manuscript preparation. J.D. is an Investigator with the Howard Hughes Medical Institute. K.H.G. gratefully acknowledges support from the University of Texas Southwestern Endowed Scholars Program.

1. Buchanan, S. K., Smith, B. S., Venkatramani, L., Xia, D., Esser, L., Palnitkar, M., Chakraborty, R., van der Helm, D. & Deisenhofer, J. (1999) *Nat. Struct. Biol.* **6,** 56–63.
2. van der Helm, D., Jalal, M. A. F. & Hossain, M. B. (1987) in *Iron Transport in Microbes, Plants and Animals*, eds. Winkelmann, G., van der Helm, D. & Neilands, J. B. (VCH, New York), pp. 135–166.
3. Llinas, M., Wilson, D. M. & Neilands, J. B. (1973) *Biochemistry* **12,** 3836–3843.
4. Mademidis, A. & Köster, W. (1998) *Mol. Gen. Genet.* **258,** 156–165.
5. Braun, V. (1995) *FEMS Microbiol. Rev.* **16,** 295–307.
6. Larsen, R. A., Foster-Hartnett, D., McIntosh, M. A. & Postle, K. (1997) *J. Bacteriol.* **179,** 3213–3221.
7. Kadner, R. J. & Heller, K. J. (1995) *J. Bacteriol.* **177,** 4829–4835.
8. Ferguson, A. D., Hofmann, E., Coulton, J. W., Diederichs, K. & Welte, W. (1998) *Science.* **282,** 2215–2220.
9. Locher, K. P., Rees, B., Koebnik, R., Mitschler, A., Moulinier, L., Rosenbusch, J. P. & Moras, D. (1998) *Cell* **95,** 771–778.
10. Killmann, H. & Braun, V. (1994) *FEMS Microbiol. Lett.* **119,** 71–76.
11. Jalal, M. A. & van der Helm, D. (1989) *FEBS Lett.* **243,** 366–370.
12. Sambrook, J., Fritsch, E. F. & Maniatis, T. (1989) *Molecular Cloning: A Laboratory Manual* (Cold Spring Harbor Lab. Press, Plainview, NY), 2nd Ed., pp. A1–A3.
13. Piotto, M., Saudek, V. & Sklenar, V. (1992) *J. Biomol. NMR* **2,** 661–665.
14. Kay, L. E., Keifer, P. & Saarinen, T. (1992) *J. Am. Chem. Soc.* **114,** 10663–10665.
15. Bashford, C. L. (1987) in *Spectrophotometry and Spectrofluorimetry, A Practical Approach*, eds. Harris, D. A. & Bashford, C. L. (IRL Press, Washington, DC), pp. 20–21.
16. Zhang, X.-J. & Matthews, B. W. (1995) *J. Appl. Crystallogr.* **28,** 624–630.
17. Chothia, C. (1976) *J. Mol. Biol.* **105,** 1–12.
18. Jones, S. & Thornton, J. M. (1995) *Prog. Biophys. Mol. Biol.* **63,** 31–65.
19. Dill, K. A. (1990) *Biochemistry* **29,** 7133–7155.
20. Greenfield, N. & Fasman, G. D. (1969) *Biochemistry* **8,** 4108–4116.
21. Fasshauer, D., Otto, H., Eliason, W. K., Jahn, R. & Brünger, A. T. (1997) *J. Biol. Chem.* **272,** 28036–28041.
22. House-Pompeo, K., Xu, Y., Joh, D., Speziale, P. & Höök, M. (1996) *J. Biol. Chem.* **271,** 1379–1384.
23. Asakura, T., Taoka, K., Demura, M. & Williamson, M. P. (1995) *J. Biomol. NMR* **6,** 227–236.
24. Penkett, C. H., Redfield, C., Dodd, I., Hubbard, J., McBay, D. L., Mossakowska, D. E., Smith, R. A. G., Dobson, C. M. & Smith, L. J. (1997) *J. Mol. Biol.* **274,** 152–159.
25. Hazzard, J., Südhof, T. C. & Rizo, J. (1999) *J. Biomol. NMR* **14,** 203–207.
26. Daughdrill, G. W., Hanely, L. J. & Dahlquist, F. W. (1998) *Biochemistry* **37,** 1076–1082.
27. McIntosh, M. A., Chenault, S. S. & Earhart, C. F. (1979) *J. Bacteriol.* **137,** 653–657.
28. Wiener, M., Freymann, D., Ghosh, P. & Stroud, R. M. (1997) *Nature (London)* **385,** 461–464.
29. Schramm, E., Mende, J., Braun, V. & Kamp, R. M. (1987) *J. Bacteriol.* **169,** 3350–3357.
30. Kraulis, P. J. (1991) *J. Appl. Crystallogr.* **24,** 946–950.
31. Merritt, E. A. & Bacon, D. J. (1997) *Methods Enzymol.* **277,** 505–524.